



# *In Silico* Analyses on the Comparative Potential of Therapeutic Human Monoclonal Antibodies Against Newly Emerged SARS-CoV-2 Variants Bearing Mutant Spike Protein

## OPEN ACCESS

### Edited by:

Uday Kishore,  
Brunel University London,  
United Kingdom

### Reviewed by:

Taruna Madan,  
National Institute for Research in  
Reproductive Health (ICMR), India  
Anthony George Tsolaki,  
Brunel University London,  
United Kingdom

### \*Correspondence:

Jagadeesh Bayry  
bayry@iitpkd.ac.in  
Suprabhat Mukherjee  
suprabhat.mukherjee@knu.ac.in;  
babaimbc@gmail.com

<sup>†</sup>These authors have contributed  
equally to this work

### Specialty section:

This article was submitted to  
Molecular Innate Immunity,  
a section of the journal  
Frontiers in Immunology

**Received:** 24 September 2021

**Accepted:** 07 December 2021

**Published:** 10 January 2022

### Citation:

Das NC, Chakraborty P, Bayry J  
and Mukherjee S (2022) *In Silico*  
Analyses on the Comparative  
Potential of Therapeutic Human  
Monoclonal Antibodies Against Newly  
Emergent SARS-CoV-2 Variants  
Bearing Mutant Spike Protein.  
*Front. Immunol.* 12:782506.  
doi: 10.3389/fimmu.2021.782506

Nabarun Chandra Das<sup>1†</sup>, Pritha Chakraborty<sup>1†</sup>, Jagadeesh Bayry<sup>2\*</sup>  
and Suprabhat Mukherjee<sup>1\*</sup>

<sup>1</sup> Integrative Biochemistry and Immunology Laboratory, Department of Animal Science, Kazi Nazrul University, Asansol, India,

<sup>2</sup> Department of Biological Sciences and Engineering, Indian Institute of Technology Palakkad, Palakkad, India

Since the start of the pandemic, SARS-CoV-2 has already infected more than 250 million people globally, with more than five million fatal cases and huge socio-economic losses. In addition to corticosteroids, and antiviral drugs like remdesivir, various immunotherapies including monoclonal antibodies (mAbs) to S protein of SARS-CoV-2 have been investigated to treat COVID-19 patients. These mAbs were initially developed against the wild-type SARS-CoV-2; however, emergence of variant forms of SARS-CoV-2 having mutations in the spike protein in several countries including India raised serious questions on the potential use of these mAbs against SARS-CoV-2 variants. In this study, using an *in silico* approach, we have examined the binding abilities of eight mAbs against several SARS-CoV-2 variants of Alpha (B.1.1.7) and Delta (B.1.617.2) lineages. The structure of the Fab region of each mAb was designed *in silico* and subjected to molecular docking against each mutant protein. mAbs were subjected to two levels of selection based on their binding energy, stability, and conformational flexibility. Our data reveal that tixagevimab, regdanvimab, and cilgavimab can efficiently neutralize most of the SARS-CoV-2 Alpha strains while tixagevimab, bamlanivimab, and sotrovimab can form a stable complex with the Delta variants. Based on these data, we have designed, by *in silico*, a chimeric antibody by conjugating the CDRH3 of regdanivimab with a sotrovimab framework to combat the variants that could potentially escape from the mAb-mediated neutralization. Our finding suggests that though currently available mAbs could be used to treat COVID-19 caused by the variants of SARS-CoV-2, better results could be expected with the chimeric antibodies.

**Keywords:** COVID-19, SARS-CoV-2, variants, spike protein, monoclonal antibody (mAb), *in silico* approach

## INTRODUCTION

The coronavirus disease 2019 (COVID-19) pandemic caused by severe acute respiratory syndrome coronavirus 2 (SARS-CoV-2) has become the biggest threat of the century to mankind with huge mortality (more than 5.1 million), socio-economic loss, and psychological issues (1–3). The causative virus SARS-CoV-2 is a spherical-shaped RNA virus surrounded by a glycoprotein envelope consisting of a crown-like spike protein alongside 27–32 kb positive sense single-stranded RNA genome (4, 5). Membrane glycoprotein (M), Nucleocapsid (N), Envelope (E), and Spike protein (S) are the crucial structural proteins of the virus while main protease and RNA-dependent RNA polymerase (RdRP) are the major non-structural proteins. Upon infection, the S glycoprotein binds to the human angiotensin converting enzyme-2 (ACE-2) receptor located mainly on the alveolar cells of the respiratory tract following the entry of the virus particles inside the host cells by the action of human transmembrane serine protease 2 (TMPRSS2) (6, 7). Moreover, the spike glycoprotein also interacts with the toll-like receptors 4 (TLR4) leading to the induction of strong proinflammatory responses in the lungs (8, 9). Induction of intense proinflammatory responses within the lungs termed “cytokine storm” is the principle cause of lung damage, multiple organ failure, and death (10, 11). Since its first report in the Wuhan province of China in December 2019, the SARS-CoV-2 has undergone a number of mutations, particularly in the S glycoprotein, resulting in the emergence of a number of variants (12) especially in UK, Europe, and India (13). Strains reported from India, namely, B.1.617 (Kappa), B.1.617.2 (Delta), and B.1.618, have been characterized as exceedingly transmissible SARS-CoV-2 variants (14). These variants possess mutations within the S protein that plays a major role in the viral infection through recognition of receptor and host cell membrane fusion (15). L452R, E484Q, D614G, and P681R mutations in the S protein have been documented in B.1.617 lineage while D145-146, E484K, and D614G mutations were prevalent in B.1.618 (14). Among these variants, the Delta strain possesses higher infectivity, mortality, and post-infection issues (16, 17). Mutant S proteins within these variants have been found to promote infectivity, transmission, and resistance to vaccine-induced immune response (18–20).

The clinical management strategy of COVID-19 primarily aims to alleviate the inflammation and the virus load. Recently, immunotherapies and antibody-based therapies targeting either the virus or virus-induced inflammation were also investigated (21–23). Several monoclonal antibodies (mAbs) like bamlanivimab, regdanvimab, tixagevimab, cilgavimab, etesevimab, casirivimab, imdevimab, and sotrovimab directed against the spike protein of SARS-CoV-2 to prevent the viral attachment and infection of host cell have been developed by several firms and are at various stages of clinical trials (24–26). These mAbs were developed against the wild-type SARS-CoV-2; however, emergence of variant forms of SARS-CoV-2 has raised questions on the efficacy of these mAbs against SARS-CoV-2 variants.

In this study, we have investigated the theoretical therapeutic efficacy of eight mAbs that are at various stages of development

or clinical trials, against twenty SARS-CoV-2 variants of two different lineages of UK (B.1.1.7, Alpha) and Indian (B.1.617.2, Delta) origin having mutation in the S protein through *in silico* approaches. Furthermore, we also hypothesized a chimeric mAb for possible application against variant SARS-CoV-2 infection.

## METHODS

### Data Mining

Mutated amino acids of spike glycoprotein of Alpha and Delta variants were retrieved from the GISAID database (<https://www.gisaid.org/>). Amino acid sequence of native spike glycoprotein (Accession ID: QHD43416.1) of SARS-CoV-2 and therapeutic mAbs were retrieved from the NCBI (<https://www.ncbi.nlm.nih.gov/>) and CoV-AbDab database (<http://opig.stats.ox.ac.uk/webapps/covabdab/>), respectively (27).

### Homology Modeling

Homology modeling is a template-dependent/independent method popularly used to model protein structure from its amino acid sequence. Based on the templates available in the database repository, an automated modeling server, SWISS-MODEL, was used to model all the mutant S proteins (28). Similarly, the web application ABodyBuilder, a tool for small-scale homology modeling (29), was applied for designing the Fv regions of the mAbs used in this study. The ABodyBuilder algorithm works through the following pathway, i.e., selection of template>prediction of orientation>prediction of the side chain>modeling of complementarity determining region loop to design computational model of the mAbs (30). Antibody i-Patch, a web tool that works on the antibody-specific statistics to determine the paratope and complementarity-determining regions (CDR) within the antibody, was also utilized to validate the efficacy of the paratopes towards an antigen (31). In addition, the webtool EpiPred was explored to determine the epitopes by using the homology model of the antibody as an input (32, 33). Each structure was verified using SAVES server that examines the stereochemical quality of a predicted protein structure through analyzing the residue-by-residue geometry and geometry of the overall structure (34, 35).

### Molecular Docking

The protein–protein interactions between the S protein variants and human mAbs were determined through molecular docking study using High Ambiguity Driven protein–protein DOCKing (HADDOCK) v. 2.4. This flexible docking program executes the docking process by using the information from known and/or predicted protein interfaces in ambiguous interaction restraints (AIR) and the outputs generated by this server were found to support experimentally validated (NMR and cryo-EM) structures of protein complexes (36). Herein, the PDB files of each SARS-CoV-2 variant and mAb were subjected to binding interactions in HADDOCK platform and the protein–protein interaction was predicted through a binding score provided by the webserver as well as analyzing the interacting residues

within the output file. All the docked complexes were analyzed for biophysical interactions using Discovery Studio-2020 and PyMOL.

## Analyses of the Molecular Basis of Protein–Protein Interactions

Stability of the molecular topology, conformational topology, and dynamic behavior of the mAb–spike protein complex was studied through normal mode analyses (NMA) (37). Different protein complexes were analyzed for molecular flexibility and modal trajectories of structural dynamics using iMODS server from ChaconLab (38). NMA is a quantitative expression of motion of protein in a complex. In our study, NMA analyses were conducted to assess the biophysical attributes of S protein–mAb complexes. The iMODS server is a popular and customizable server that discloses coarse-grain (CG) levels and also determines the dihedral coordinates of C-alpha atoms in the proteins. iMod also delivers an NMA mobility that illustrates the collective motions and affine-model arrows that direct domain dynamics. Structural deformability usually depends on the helical content of a protein that is usually studied by analyzing the *B*-factor (39). Here, we studied the amplitude of atomic displacement in each spike protein–mAb complex by determining the *B*-factor. The relative impact of each deformation movement in the motion of interacting proteins within the S protein–mAb complex was studied by measuring the eigenvalues. Lower eigenvalues are indicative of greater stability while higher values reveal the reverse (4). The molecular flexibility, amplitude of fluctuation of each mode, and overall conformational change in each S protein–mAb complex were studied by variance plot and covariance matrix. The docked complexes comprising S protein variants and mAbs were prepared in pdb format and submitted to the iMODS server to determine the normal modes within internal coordinates and details of the mobility (*B*-factor), structural deformability, covariance map, and linking matrix with eigenvalues. The data extracted from iMODS were analyzed and plotted using the statistical software package R. Changes in the conformation in S protein after binding of mAb were assessed by superimposing the unbound S protein structures on the S protein–mAb complex following our earlier reports (9, 39).

Selected variant S proteins of SARS-CoV-2 and the therapeutic mAbs were examined utilizing PRODIGY web tool to determine its binding affinity ( $\Delta G$ ) and dissociation constant ( $K_d$ ) (40).

## Designing of Chimeric Antibody

The rationale behind using *in silico* docking analysis was to check the binding efficacy of the mAbs against the S protein variants. The clear demonstration of the biomolecular interaction among S protein variants and mAbs was possible only through molecular docking. Hence, it was necessary to screen the possible efficacious mAbs and to obtain a precise picture on their respective CDRs to predict the possible interacting domains present in those antibodies. Such CDRs are important components of the chimeric antibody generated *in silico*.

After identifying the potential CDR patches in the screened mAbs, a series of chimeric antibodies were hypothesized for better efficacy. The binding domain of the mAbs were subjected to multiple sequence alignment and the peptide fragments showing binding affinity against SARS-CoV-2 variants were combined *in silico*. The resultant CDRs were fitted in a single amino acid chain to model the antibody structure by employing Therapeutic Antibody Profiler (TAP) (41, 42). The designed chimeric antibody was characterized for its immune-biological properties and efficacy against the S protein *in silico*.

## RESULTS

This study seeks to determine the efficacy of various human mAbs reported to date for their binding to S proteins of SARS-CoV-2 Alpha and Delta variants.

### Screening of Efficacious mAbs Against Spike Protein Variants

For all the eight mAbs, 10 spike protein variants from Alpha and 10 from Delta lineages (shown in **Figure S1**) were tested for all possible interactions *in silico* (**Table S1**). A total of 160 mAb–spike protein complexes were obtained using Haddock 2.4 and were further screened by setting the docking score >100 as strong interaction while <50 as weak interaction (43). With these criteria, we studied 3 strong and 3 weak spike protein–mAb complexes for each mAb. The rationale behind such a selection was to filter the mAbs that are effective against a greater number of SARS-CoV-2 variants and also to understand the possible variants that could escape binding of the mAb. Regdanvimab, bamlanivimab, sotrovimab, etesevimab, and cilgavimab showed high docking scores against most of the Alpha and Delta variants (**Figure S2**). Particularly, regdanvimab displayed a high binding score against both Alpha and Delta variants. In contrast, tixagevimab, casirvimab, imdevimab, and cilgavimab possessed less docking scores. Docking score is a preliminary measurement of binding efficacy of the mAbs against the SARS-CoV-2 variants, and therefore, to validate the initial postulation as well as to obtain molecular insight on these interactions, we further refined our screening by including a total of 16 protein complexes comprising S protein variants from the Alpha lineage and 8 mAbs (**Table S1**). This was repeated for the Delta lineage.

### Comparative Analyses of the Biomolecular Interactions Between the mAbs and Spike Protein Variants and Studies on the Molecular Dynamics

The biophysical basis of mAb–SARS-CoV-2 spike protein interactions was investigated through determining the binding free energy and binding affinity. Eventually, three strongly bound and three weakly bound protein complexes were selected from each lineage (**Table 1**). P681H–tixagevimab, S982A–regdanvimab, and V70–cilgavimab complexes displayed significantly strong binding interactions with respective binding free energy ( $\Delta G$ ) of  $-15.1$ ,  $-14.7$ , and  $-14.7$  kcal/mol.

**TABLE 1** | Comparative analyses of the biophysical interactions (binding energy and binding affinity) between the mutated spike protein from SARS-CoV-2 variants and human mAbs.

| Lineage of SARS-CoV-2 Strain | Spike protein with mutation | Bind with monoclonal antibody | Haddock score          | Binding affinity $\Delta G$ (kcal/mol) | Dissociation constant $K_d$ (M) at 25.0°C |                |
|------------------------------|-----------------------------|-------------------------------|------------------------|--|---|----------------|
| B.1.1.7<br>(Alpha)           | P681H                       | Bamlanivimab                  | Strongly docked        | $-104.8 \pm 6.4$                       | -11.9                                     | 1.9E-09        |
|                              | D1118H                      |                               | Weakly docked          | $-38.0 \pm 10.3$                       | -12.4                                     | 7.7E-10        |
|                              | <b>S982A</b>                | <b>Regdanvimab</b>            | <b>Strongly docked</b> | $-142.8 \pm 4.1$                       | <b>-14.7</b>                              | <b>1.6E-11</b> |
|                              | T716I                       |                               | Weakly docked          | $-103.5 \pm 6.8$                       | -13.3                                     | 1.8E-10        |
|                              | <b>P681H</b>                | <b>Tixagevimab</b>            | <b>Strongly docked</b> | $-94.0 \pm 7.6$                        | <b>-15.1</b>                              | <b>7.8E-12</b> |
|                              | <b>S982A</b>                |                               | <b>Weakly docked</b>   | $-20.4 \pm 6.5$                        | <b>-11.1</b>                              | <b>6.7E-09</b> |
|                              | <b>V70-</b>                 | <b>Cilgavimab</b>             | <b>Strongly docked</b> | $-87.9 \pm 7.5$                        | <b>-14.7</b>                              | <b>1.6E-11</b> |
|                              | <b>T716I</b>                |                               | <b>Weakly docked</b>   | $-61.5 \pm 6.1$                        | <b>-8.7</b>                               | <b>4.2E-07</b> |
|                              | D614G                       | <b>Etesevimab</b>             | Strongly docked        | $-139.0 \pm 3.2$                       | -10.9                                     | 1.1E-08        |
|                              | <b>S982A</b>                |                               | <b>Weakly docked</b>   | $-51.0 \pm 3.2$                        | <b>-12.2</b>                              | <b>1.1E-09</b> |
|                              | H69-                        | Casirivimab                   | Strongly docked        | $-72.5 \pm 5.0$                        | -13.8                                     | 7.5E-11        |
|                              | Y144-                       |                               | Weakly docked          | $-33.3 \pm 1.9$                        | -13.1                                     | 2.6E-10        |
|                              | V70-                        | Imdevimab                     | Strongly docked        | $-76.6 \pm 5.1$                        | -9.9                                      | 5.3E-08        |
|                              | T716I                       |                               | Weakly docked          | $-34.9 \pm 11.8$                       | -14.4                                     | 2.8E-11        |
|                              | D1118H                      | Sotrovimab                    | Strongly docked        | $-132.2 \pm 15.4$                      | -14.1                                     | 4.6E-11        |
| D614                         |                             | Weakly docked                 | $-67.1 \pm 14.4$       | -13.0                                  | 2.8E-10                                   |                |
| B.1.617.2<br>(Delta)         | <b>P681R</b>                | <b>Bamlanivimab</b>           | <b>Strongly docked</b> | $-106.3 \pm 5.4$                       | <b>-14.1</b>                              | <b>4.7E-11</b> |
|                              | <b>T19R</b>                 |                               | <b>Weakly docked</b>   | $-50.0 \pm 13.3$                       | <b>-10.0</b>                              | <b>4.4E-08</b> |
|                              | D614G                       | <b>Regdanvimab</b>            | Strongly docked        | $-140.3 \pm 3.1$                       | -10.7                                     | 1.4E-08        |
|                              | <b>T19R</b>                 |                               | <b>Weakly docked</b>   | $-117.8 \pm 10.6$                      | <b>-10.6</b>                              | <b>1.6E-08</b> |
|                              | <b>P681R</b>                | <b>Tixagevimab</b>            | <b>Strongly docked</b> | $-90.4 \pm 4.0$                        | <b>-13.9</b>                              | <b>6.9E-11</b> |
|                              | <b>G142D</b>                |                               | <b>Weakly docked</b>   | $-22.6 \pm 10.3$                       | <b>-10.2</b>                              | <b>3.1E-08</b> |
|                              | E156G                       | Cilgavimab                    | Strongly docked        | $-112.2 \pm 11.4$                      | -12.4                                     | 8.1E-10        |
|                              | D614G                       |                               | Weakly docked          | $-66.1 \pm 17.2$                       | -11.5                                     | 3.5E-09        |
|                              | D614G                       | Etesevimab                    | Strongly docked        | $-139.0 \pm 3.2$                       | -10.9                                     | 1.1E-08        |
|                              | R158-                       |                               | Weakly docked          | $-38.9 \pm 18.9$                       | -13.4                                     | 1.6E-10        |
|                              | T478K                       | Casirivimab                   | Strongly docked        | $-74.9 \pm 5.0$                        | -12.0                                     | 1.5E-09        |
|                              | G142D                       |                               | Weakly docked          | $-37.3 \pm 9.3$                        | -12.9                                     | 3.5E-10        |
|                              | P681R                       | Imdevimab                     | Strongly docked        | $-82.6 \pm 5.3$                        | -13.1                                     | 2.3E-10        |
|                              | T19R                        |                               | Weakly docked          | $-37.7 \pm 16.9$                       | -11.0                                     | 7.9E-09        |
|                              | <b>R158-</b>                | <b>Sotrovimab</b>             | <b>Strongly docked</b> | $-132.0 \pm 7.9$                       | <b>-13.3</b>                              | <b>1.6E-10</b> |
| D614G                        |                             | Weakly docked                 | $-67.1 \pm 14.4$       | -13.0                                  | 2.8E-10                                   |                |

*Bold values are depicting the 3 strongly and 3 weakly docked structure.*

Analysis of binding affinity in terms of the dissociation constant ( $K_d$ ) supported the inference of binding energy. The data revealed that P681H-tixagevimab, S982A-regdanvimab, and V70-cilgavimab possess  $K_d$  values of 7.8E-12, 1.6E-11, and 1.6E-11 respectively. These data suggested that tixagevimab, regdanvimab, and cilgavimab could efficiently bind to the SARS-CoV-2 variants of B.1.1.7 lineage. In contrast, weak interactions were noted for S982A-tixagevimab, T716I-cilgavimab, and S982A-etesevimab, indicating that the variants with spike protein mutations like S982A could escape the inhibitory effect of certain mAbs.

For B.1.617.2 lineage, P681R-bamlanivimab, P681R-tixagevimab, and R158-sotrovimab complexes revealed strong interactions with respective binding free energies ( $\Delta G$ ) of -14.1, -13.9, and -13.3 kcal/mol. Furthermore, SARS-CoV-2 that harbors S protein mutations T19R and G142D were predicted as the variants that could escape from the inhibitory effects of aforesaid mAbs.

Taking clues from earlier studies, the top three strongly bound and three weakly bound mAb-spike protein variant complexes from each lineage were studied for protein-protein interactions at the molecular level (Table 1). The topological differences in binding pattern of different mAbs to S protein

variants as well as involvement of various non-covalent bonds/forces are summarized in Figure S3 and Table 2. While studying the most strongly bound complex for the B.1.1.7 lineage, the P681H-tixagevimab complex was found to be stabilized by the most number (a total of 26 H-bonds) of hydrogen bonds. In addition, hydrophobic interaction ( $\pi$ -Alkyl: 1) was found to provide additional stability in holding the two proteins (Figure S3A and Table 2). The other strongly bound complexes, viz., S982A-regdanvimab and V70-cilgavimab, were also found to possess similar numbers of H-bonds. However, additional interactive forces (4 hydrophobic interactions;  $\pi$ -Alkyl: 3 and alkyl: 1; and electrostatic bonds: 2) were noted in V70-cilgavimab (Figure S3B and Table 2). However, the topology of binding was dissimilar (as evident from the interacting amino acids) to that of tixagevimab and that could explain the reduced binding affinity. In comparison to the high-affinity antibodies, we found lesser degree of interactions in terms of hydrogen bonding and/or other noncovalent interactions leading to weak binding of mAb to S variants as evident for T716I-cilgavimab, S982A-tixagevimab, and S982A-etesevimab (Figures S3A, B and Table S3).

Biomolecular interactions between mAbs and S protein variants were also studied for the B.1.617.2 lineage. P681R-

**TABLE 2 |** Biomolecular interactions amongst the spike proteins and high affinity monoclonal antibodies.

| Interaction details  |              |   |              |                          |              |   |              |                        |              |   |              |
|--|--------------|---|--------------|--------------------------|--------------|---|--------------|------------------------|--------------|---|--------------|
| Antigen residues   | Fab residues | Matched with SAbPred predicted CDR residues | Distance (Å) | Antigen residues         | Fab residues | Matched with SAbPred predicted CDR residues | Distance (Å) | Antigen residues       | Fab residues | Matched with SAbPred predicted CDR residues | Distance (Å) |
| <b>B.1.1.7 (Alpha) -Lineage of SARS-CoV-2 Strain</b>         |              |   |              |                          |              |   |              |                        |              |   |              |
| <b>P681H-tixagevimab</b>                                     |              |   |              | <b>S982A-regdanvimab</b> |              |   |              | <b>V70-cilgavimab</b>  |              |   |              |
| <b>Hydrogen Bond</b>   |              |   |              |                          |              |   |              |                        |              |   |              |
| GLY472   | ARG44        |   | 1.846        | ASP3092                  | LYS66        |   | 1.57546      | ASP2610                | LEU109       | Y   | 1.68776      |
| SER1561  | ASN57        | Y   | 2.20629      | ASP2536                  | LYS73        |   | 2.66857      | TYR1565                | LYS150       | Y   | 2.38416      |
| TYR436   | ARG67        |   | 3.07872      | LYS2527                  | ASP56        | Y   | 3.21068      | SER2617                | SER154       | Y   | 1.79876      |
| VAL1485  | GLU122       |   | 2.11712      | LYS2527                  | ASP56        | Y   | 1.56226      | GLU2586                | TYR157       | Y   | 1.73972      |
| VAL1485  | GLN148       | Y   | 2.99581      | ASN2852                  | GLY33        | Y   | 2.24497      | GLU2586                | SER159       | Y   | 1.74693      |
| VAL1485  | GLN148       | Y   | 2.88623      | ASN2529                  | LYS59        |   | 1.70743      | GLY1601                | LYS162       | Y   | 2.56925      |
| CYS1454  | SER149       | Y   | 2.03091      | GLU2530                  | HIS61        |   | 2.14448      | PHE1602                | LYS162       | Y   | 1.95827      |
| GLU1458  | SER151       | Y   | 1.74429      | ASN1674                  | THR67        |   | 1.87769      | GLY1601                | THR185       | Y   | 1.82372      |
| ALA1462  | SER215       | Y   | 1.80752      | GLN749                   | TYR105       | Y   | 2.44674      | GLN1609                | SER199       |   | 2.6446       |
| SER1489  | ARG217       | Y   | 2.63386      | ASP3079                  | TYR107       | Y   | 2.91451      | PHE2584                | SER159       | Y   | 2.89539      |
| SER1489  | ARG217       | Y   | 1.73988      | LYS3074                  | TYR155       | Y   | 2.47154      | GLY2585                | SER159       | Y   | 1.78483      |
| ASN435   | GLU66        |   | 2.6411       | ASN3073                  | ASN174       | Y   | 2.37936      | ASN2589                | TYR224       | Y   | 2.07595      |
| GLN480   | GLN62        |   | 2.88996      | SER3189                  | LYS176       | Y   | 2.19465      | ASN2616                | SER199       |   | 1.97765      |
| PHE484   | GLU66        |   | 1.83268      | ASN3073                  | LYS189       |   | 1.98564      | LYS2632                | PRO108       | Y   | 2.21217      |
| ASN488   | GLU66        |   | 3.0399       | ASP3069                  | GLY191       |   | 2.45689      | GLY1601                | SER184       | Y   | 3.01655      |
| GLY1457  | SER149       | Y   | 2.53091      | LYS2527                  | ASN58        | Y   | 1.92671      | GLY1612                | GLU202       |   | 3.33806      |
| ASN1461  | GLY214       | Y   | 2.5667       | LYS2527                  | ASP56        | Y   | 3.08543      | THR2631                | PRO108       | Y   | 3.25262      |
| ASN1461  | ARG217       | Y   | 2.01651      | THR2535                  | ASP57        | Y   | 1.62597      |                        |              |   |              |
| THR1463  | TYR154       | Y   | 1.85134      | ASN2852                  | GLY33        | Y   | 2.40857      |                        |              |   |              |
| ARG1464  | SER216       | Y   | 2.74405      | ASN3073                  | LYS189       |   | 2.52172      |                        |              |   |              |
| ASN1488  | GLU122       |   | 1.77181      | LEU3077                  | ASN153       | Y   | 2.01706      |                        |              |   |              |
| SER1489  | GLU122       |   | 1.84294      | ALA3078                  | ASN153       | Y   | 2.00835      |                        |              |   |              |
| LEU1453  | SER149       | Y   | 3.22639      | GLN3198                  | ASN106       | Y   | 2.43996      |                        |              |   |              |
| GLU1458  | SER151       | Y   | 3.29199      | SER3188                  | LYS176       | Y   | 3.40308      |                        |              |   |              |
| ASN1461  | SER215       | Y   | 3.02321      | ASP3069                  | SER190       |   | 3.14642      |                        |              |   |              |
| GLY434   | GLU66        |   | 3.41544      | SER3188                  | ASN175       | Y   | 3.32419      |                        |              |   |              |
| PRO1455  | SER149       | Y   | 2.95993      | GLN3259                  | TYR105       | Y   | 3.59512      |                        |              |   |              |
| <b>Electrostatic Bond</b>                                    |              |   |              |                          |              |   |              |                        |              |   |              |
|  |              |   |              | GLU2530                  | LYS59        |   | 4.65638      |                        |              |   |              |
|  |              |   |              | LYS3074                  | ASP173       | Y   | 4.51837      |                        |              |   |              |
| <b>Hydrophobic Bond (<math>\pi</math>-Alkyl)</b>             |              |   |              |                          |              |   |              |                        |              |   |              |
| TYR436   | ARG67        |   | 5.06439      | ALA753                   | TYR105       | Y   | 4.49149      |                        |              |   |              |
|  |              |   |              | VAL995                   | TYR105       | Y   | 5.34089      |                        |              |   |              |
|  |              |   |              | LEU999                   | TYR105       | Y   | 5.42826      |                        |              |   |              |
| <b>Hydrophobic Bond (Alkyl)</b>                              |              |   |              |                          |              |   |              |                        |              |   |              |
|  |              |   |              | ALA3094                  | LYS66        |   | 4.76062      |                        |              |   |              |
| <b>Hydrophobic Bond (<math>\pi</math>- <math>\pi</math>)</b> |              |   |              |                          |              |   |              |                        |              |   |              |
|  |              |   |              |                          |              |   |              | PHE1602                | TRP182       | Y   | 5.46997      |
| <b>B.1.617.2 (Delta)-Lineage of SARS-CoV-2 Strain</b>        |              |   |              |                          |              |   |              |                        |              |   |              |
| <b>P681R-bamlanivimab</b>                                    |              |   |              | <b>P681R-tixagevimab</b> |              |   |              | <b>R158-sotrovimab</b> |              |   |              |
| <b>Hydrogen Bond</b>   |              |   |              |                          |              |   |              |                        |              |   |              |
| GLU327   | ARG50        |   | 1.55363      | GLY2734                  | ARG44        |   | 2.24393      | ASP1955                | ARG141       |   | 2.77667      |
| GLU327   | ARG50        |   | 2.39339      | SER430                   | ASN57        | Y   | 2.58051      | ALA1804                | THR74        | Y   | 3.03559      |
| GLY326   | ARG50        |   | 2.56527      | TYR2698                  | ARG67        |   | 2.59736      | ALA3012                | TRP104       | Y   | 2.57857      |
| ASP351   | HIS104       | Y   | 1.69139      | VAL354                   | GLN148       | Y   | 2.61321      | GLN2118                | SER106       | Y   | 2.67731      |
| GLU327   | TYR106       | Y   | 1.75457      | CYS323                   | SER149       | Y   | 2.2566       | THR2122                | SER106       | Y   | 1.89863      |
| GLU2733  | SER178       | Y   | 2.35228      | GLU327                   | SER151       | Y   | 1.7445       | GLU1397                | SER154       | Y   | 2.77409      |
| CYS323   | ALA103       | Y   | 2.90251      | ASN330                   | SER215       | Y   | 1.99254      | ASN1940                | ARG169       |   | 1.84746      |
| PHE325   | TYR106       | Y   | 2.80316      | SER358                   | ARG217       | Y   | 2.25764      | ALA1945                | ARG178       | Y   | 1.6848       |
| GLY326   | TYR106       | Y   | 1.86565      | PHE325                   | SER149       | Y   | 3.07747      | ALA1945                | ARG178       | Y   | 2.44364      |
| GLN2747  | SER152       | Y   | 2.014        | GLY326                   | SER149       | Y   | 2.37639      | THR1943                | THR180       | Y   | 1.79555      |
| ASN2750  | TYR214       | Y   | 2.35522      | ASN330                   | ARG217       | Y   | 1.68917      | VAL1942                | GLY181       |   | 2.30551      |
| SER358   | TYR105       | Y   | 3.23675      | THR332                   | TYR154       | Y   | 2.34097      | ASP1959                | GLY190       |   | 1.69436      |
| GLN2747  | SER150       | Y   | 3.24228      | ARG333                   | SER216       | Y   | 2.09294      | THR1720                | SER31        | Y   | 1.80176      |

(Continued)

TABLE 2 | Continued

| Interaction details  |              |   |              |                  |              |   |              |                  |              |   |              |
|--|--------------|---|--------------|------------------|--------------|---|--------------|------------------|--------------|---|--------------|
| Antigen residues   | Fab residues | Matched with SAbPred predicted CDR residues | Distance (Å) | Antigen residues | Fab residues | Matched with SAbPred predicted CDR residues | Distance (Å) | Antigen residues | Fab residues | Matched with SAbPred predicted CDR residues | Distance (Å) |
| TYR2698  | SER152       | Y   | 3.42903      | ASN357           | GLU122       |   | 1.83192      | GLN1723          | TYR54        | Y   | 2.02886      |
| GLY2695  | GLY190       |   | 3.73547      | SER358           | GLU122       |   | 3.08345      | GLN2065          | GLY103       | Y   | 1.89888      |
| GLY2745  | SER152       | Y   | 3.47513      | VAL432           | ASN57        | Y   | 2.96427      | ASN2069          | ARG102       | Y   | 2.14298      |
|  |              |   |              | TYR2698          | GLN65        |   | 2.69082      | GLN3008          | SER106       | Y   | 2.1518       |
|  |              |   |              | TYR2698          | GLU66        |   | 1.70023      | PHE1939          | GLY181       |   | 3.64089      |
|  |              |   |              | ASN2750          | GLU66        |   | 3.06276      | THR1720          | THR30        | Y   | 3.11702      |
|  |              |   |              | ASN2750          | GLU66        |   | 2.85583      | SER2119          | SER106       | Y   | 3.10337      |
|  |              |   |              | LEU322           | SER149       | Y   | 3.40152      | ARG1963          | SER176       |   | 1.98702      |
|  |              |   |              | ASN330           | SER215       | Y   | 2.94661      |                  |              |   |              |
|  |              |   |              | PRO324           | SER149       | Y   | 2.94922      |                  |              |   |              |
|  |              |   |              | GLY2745          | GLU66        |   | 3.14184      |                  |              |   |              |
| <b>Electrostatic Bond</b>                                      |              |   |              |                  |              |   |              |                  |              |   |              |
| GLU327   | ARG50        |   | 5.30159      |                  |              |   |              | ASP1955          | ARG141       |   | 5.484        |
|  |              |   |              |                  |              |   |              | ASP1964          | ARG178       | Y   | 4.58879      |
|  |              |   |              |                  |              |   |              | LYS1927          | GLU205       |   | 5.0261       |
| <b>Hydrophobic Bond (<math>\pi</math>-<math>\sigma</math>)</b> |              |   |              |                  |              |   |              |                  |              |   |              |
| VAL354   | HIS104       | Y   | 3.69105      |                  |              |   |              |                  |              |   |              |
| SER358   | TYR105       | Y   | 3.50298      |                  |              |   |              |                  |              |   |              |
| <b>Hydrophobic Bond (<math>\pi</math>-<math>\pi</math>)</b>    |              |   |              |                  |              |   |              |                  |              |   |              |
| PHE2735  | TYR100       | Y   | 5.22663      |                  |              |   |              |                  |              |   |              |
| <b>Hydrophobic Bond (Alkyl)</b>                                |              |   |              |                  |              |   |              |                  |              |   |              |
| LEU322   | ALA103       | Y   | 4.80066      |                  |              |   |              | PRO1928          | PRO204       |   | 4.27859      |
|  |              |   |              |                  |              |   |              | ALA1945          | ARG178       | Y   | 4.16232      |
|  |              |   |              |                  |              |   |              | ALA2058          | VAL2         |   | 4.96639      |
| <b>Hydrophobic Bond (<math>\pi</math>-Alkyl)</b>               |              |   |              |                  |              |   |              |                  |              |   |              |
| VAL354   | TYR101       | Y   | 4.57784      | TYR2698          | ARG67        |   | 5.21088      | ALA3012          | TRP104       | Y   | 5.08227      |
| VAL354   | TYR105       | Y   | 5.04138      |                  |              |   |              | ALA3258          | TRP104       | Y   | 5.01111      |
|  |              |   |              |                  |              |   |              | ALA3012          | TRP104       | Y   | 5.48531      |
|  |              |   |              |                  |              |   |              | PHE1939          | PRO183       |   | 5.48537      |

bamlanivimab, P681R-tixagevimab, and R158-sotrovimab displayed a strong binding as evidenced from their respective binding free energy (Table 1, Figures S3C, D and Tables 2 and S3). Considering the topology of binding (Figure S3C), bamlanivimab exhibited a very strong binding with S protein variant P681R, and this binding was stabilized by 16 H bonding, 1 electrostatic interaction, and 6 hydrophobic interactions ( $\pi$ - $\sigma$ : 2;  $\pi$ - $\pi$ : 1;  $\pi$ -Alkyl: 2 and alkyl: 1). Interestingly, tixagevimab was also found to interact with the same variant with a similar binding topology but with less affinity than that of bamlanivimab (Figure S3C). The abundance of H-bonds was also similar, and hence, lesser number of hydrophobic interactions could be responsible for the differences in the avidity of tixagevimab and bamlanivimab, while sotrovimab possessed strong affinity to the R158 variant and this interaction was found to be stabilized by non-covalent forces including H-bonding (Table 2). Weak interactions were observed for T19R-bamlanivimab, G142D-tixagevimab, and T19R-regdanvimab (Figure S3D and Table S3).

We scrutinized the conformational changes in S1 protein following its binding to mAb. Changes in the conformation of heterotrimeric S1 protein after binding of an antibody is key for the neutralization of SARS-CoV-2 (44). We observed clear changes in the conformation of S protein variants following

interaction with the strongly binding mAbs (Figure S4A). This observation supports the earlier data that demonstrated that tixagevimab is the strongest neutralizing mAb against SARS-CoV-2 variants. However, binding of cilgavimab to T716I revealed no sign of conformational changes and indicated that T716I could evade cilgavimab (Figure S4B). The mode of binding of mAbs and subsequent changes in the conformation were also verified by comparing tixagevimab-P681H and cilgavimab-T716I protein complexes as well as a superimposed form of them (Figure S4C).

We have also studied the molecular dynamics of S protein-mAb complexes. The comparative analyses of molecular dynamics of the most stable S protein-mAb complex, i.e., P681H-tixagevimab, and the weakest bound complex, i.e., T716I-cilgavimab, revealed significant differences in various intramolecular and intermolecular parameters (Figure S5). Clear difference in the direction of molecular motion was observed between the two protein complexes (Figures S5A-F). A relatively lower level of deformability described the compactness of P681H-tixagevimab while the reverse was observed for T716I-cilgavimab. Furthermore, protein components in the T716I-cilgavimab complex had higher mobility, indicating weak association, while the P681H-tixagevimab complex had lesser mobility, thus denoting the

strong association between components of the complex (**Figures S5E, F**). Eigenvalue is a measure of deformation due to fluctuation in protein motion (38). A high eigenvalue is indicative of a localized displacement while low eigenvalue indicates cumulative conformational changes in the protein structure (38, 39). A low eigenvalue of  $3.407305e^{-05}$  for P681H-tixagevimab revealed lower energy deformation of the structure resulting in greater stability of the complex and conformational changes in the S protein after forming complex with mAb (**Figure S5G**). In contrast, T716I-cilgavimab displayed the reverse characteristics and interpreted as relatively unstable complex.

Structural integrity of the S protein-mAb was also investigated by molecular flexibility by measuring the theoretical fluctuation (variance) of each mode in a protein complex (37). A higher degree of flexibility was observed for P681H-tixagevimab, suggesting a higher affinity of two proteins towards each other while the reverse was observed for T716I-cilgavimab (**Figures S5I, J**). Covariance maps demonstrated abundance of correlated motions of C $\alpha$  atoms in P681H-tixagevimab, thus indicating motion stiffness and rigidity in the protein complex compared to T716I-cilgavimab (**Figures S5K, L**).

## Designing of Chimeric mAb as Potential Broad-Spectrum Immunotherapeutics

Our *in silico* analyses predicted that a number of S protein variants depict very weak binding to mAbs, and therefore, these mAbs might not be effective against newly emerged strains especially Delta plus strain (B.1.617.2.1). This has prompted us to design a chimeric mAb that could be effective in encountering most of the variants (**Table S3**). We have combined the CDRs of the strongly interactive mAb to prepare a series of chimeric mAbs and tested against the spike protein variants (**Tables S3 and S4A, B**). Eventually, when we incorporated CDRH3 of regdanvimab (ARIPGFLRYRNRYYYGMDV) within the framework of sotrovimab without hampering its CDR (ARDYTRGAWFGESLIGGFND), the resultant paratope was found to display very strong binding with most of the escape variants from both lineages (**Figures 1A–C and Table S5**). Even the physico-biochemical properties, like solubility and hydrophobicity of the selected chimeric mAb, supported its durability in neutralizing the variants (**Table S6**). When we compared the efficacy of this mAb against the newly found Delta plus strain (B.1.617.2.1) and Beta strain (B.1.351), a very satisfactory binding interaction was observed as compared to the eight therapeutic mAbs (**Figure 1C and Table S7**). However, binding efficacy of the chimeric antibody against Gamma strain (P.1) was comparatively lower than that of the Delta, Delta plus, and Beta strain (**Figure 1C, Tables S5 and S7**).

## DISCUSSION

Within a year of its outbreak, SARS-CoV-2 has undergone various mutations leading to the emergence of a number of

variants with altered antigenicity and virulence. The B.1.1.7 lineage constituting the Alpha variants was first detected in UK in September 2020 and later spread to as many as 50 countries including India (45). The B.1.617 lineage was first detected in India in March 2021, and this lineage constitutes three subtypes, viz., B.1.617.1, B.1.617.2, and B.1.617.3 (46). The B.1.617.2 sub-lineage is the most virulent strain and named as Delta variant (46). High transmission rate has been the major trait of Alpha strains while Indian strains especially the Delta strains are characterized by high infectivity, severity of infection, and mortality.

S protein is the major pathogenic protein of SARS-CoV-2. In addition to attachment and infection, the S protein-TLR4 interaction is known to promote macrophage activation syndrome, acute respiratory distress syndrome, and cytokine storm leading to multi-organ damage (44, 47). Therefore, S protein is currently the major target for developing various prophylaxis and therapeutic strategies. Interestingly, several mAbs have been developed to block S protein interaction with the host receptor and to prevent the infection. Recent reports have depicted the success of some of these human mAbs in combating COVID-19 (48–50). Clinical trials supported the emergency use authorization (EUA) of bamlanivimab for treating COVID-19 patients (Coronavirus (COVID-19) Update, 2021). However, this EUA has been revoked by the Food and Drug Administration (FDA) due to the emergence of bamlanivimab resistance (51). Bamlanivimab in combination with etesevimab was reported to cause a sharp decline in the viral load as well as immunopathological consequences (21, 51). Currently bamlanivimab and etesevimab are considered as investigational drugs and are yet to receive EUA (21). Casirivimab-imdevimab combinational therapy also received EUA and clinical trials revealed satisfactory reduction in the viral load and severity of lung disease after treatment (21). This mAb combination induces phagocytosis of the infected cells through antibody-mediated cytotoxicity (11). EUA-approved sotrovimab targets the highly conserved epitope of the receptor binding domain (RBD) of the S spike protein and blocks the attachment of S protein to ACE2 (52). While regdanvimab displays strong neutralizing activity against the Delta variant with 100% survival rate in pre-clinical studies, phase III clinical data revealed reduction in the COVID-19-related hospitalization, death, and/or reduction in the recovery time of high-risk patients (53–55).

Our study presents a comparative efficacy of eight human mAbs for their binding to RBD of S glycoprotein from Alpha and Delta variants of SARS-CoV-2. Newly emerged strains have distinct host-virus interaction properties due to the occurrence of mutations in the RBD of S protein (6). Our initial binding analyses indicated that regdanvimab, bamlanivimab, sotrovimab, etesevimab, and cilgavimab could be considered for treating both Alpha and Delta strains. While comparing the response, we found that Delta strains are more responsive to the mAbs. This is a very interesting finding as most of the Delta variants reported so far could evade either wild-type SARS-CoV-2 infection-induced or vaccine-induced antibodies (14, 16). Our *in silico*

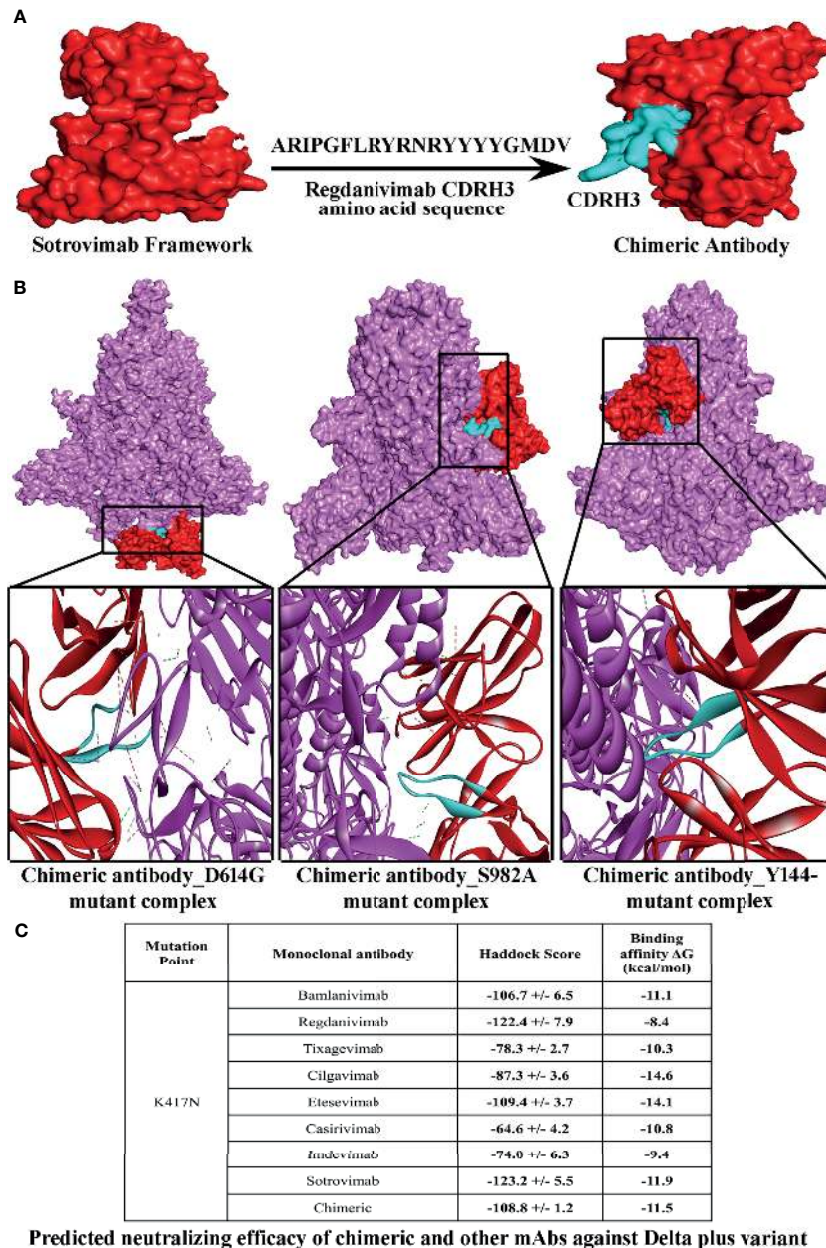


**FIGURE 1** | Structure of a chimeric mAb for inducing high-affinity binding against the greatest number of SARS-CoV-2 spike protein variants. **(A)** Depicts steps involved in the conception of a chimeric mAb. **(B)** Visualization of interactions of chimeric mAb with 3 variants of SARS-CoV-2 spike protein, namely, D614G, S982A, and Y144-. **(C)** Predicted neutralizing efficacy of chimeric and other mAbs against Delta plus variant.

studies collectively suggested that tixagevimab, regdanivimab, and cilgavimab could be the therapeutic choices for Alpha strains (B.1.1.7), while bamlanivimab, tixagevimab, and sotrovimab could be used for treating the Delta variants (B.1.617.2). Considering the *in silico* data against both B.1.1.7 and B.1.617.2 lineages, tixagevimab has been predicted to be the most potential mAb.

Conformational change is an important parameter in antigen-antibody interaction (56). We documented the

changes in S protein conformation after binding of tixagevimab, and this change in configuration was found stable after analyzing the protein motion through molecular dynamics of the tixagevimab-S protein complex. Such a stable conformational change was absent in the S protein of the escape strains. In fact, a large number of both Alpha and Delta strains were found to evade the mAbs. Therefore, we attempted to develop a chimeric antibody that could neutralize the escaping strains of both Alpha and Delta lineages including the very



recently emerged Delta plus strain. A chimeric antibody prepared using the framework of sotrovimab and the CDRH3 of regdanivimab could provide very efficient binding against most of the escape strains of Alpha, Delta, and Delta plus strains. Moreover, the binding efficiency of the chimeric antibody was found to be higher than each constituent mAb and the other six mAbs included in this study. Therefore, transformation of these predictive lines of evidence to further application level through experimental validation is expected to provide an excellent strategy to combat the emerging lethal strains of SARS-CoV-2.

In this *in silico* study, we have used several human therapeutic mAbs that were developed for treating COVID-19 (22, 57). Clinical trials of Celltrion's regdanivimab and sotrovimab from GSK and Vir Biotechnology showed their efficacy in neutralizing the SARS-CoV-2 variants of B.1.617 and B.1.1.7 lineages (58). Therefore, combining both mAbs to generate a chimeric antibody could be an attractive option to target newly emerging SARS-CoV-2 variants. In this context, rationally designed chimeric antibodies comprising an IgG1 framework with ACE2 units grafted on the CDR patches have been designed for efficient binding and neutralization of SARS-CoV-2 variants. In addition, a fusion protein called ACE2-Ig by connecting the extracellular domain of ACE2 to the Fc region human IgG1 has also been designed. This fusion protein was experimentally validated under *in vitro* conditions and found to exhibit a high degree of cross-reactivity against SARS-CoV and SARS-CoV-2 (59, 60).

Conception of therapeutic strategies *via in silico* approaches, especially identification of antigenic proteins/epitopes, designing of antibodies and vaccines, and development of new drugs and drug targets are in the current trends. To date, immunoinformatics and computational structural biology have been successfully implicated in engineering a number of efficacious immunotherapeutic agents including vaccines, chimeric antibodies, and mAbs for treating various infectious and inflammatory diseases of human (61–74). In this context, a theoretical design study by Pelat et al. (75) has demonstrated germ-line humanization of a non-human primate antibody fragment, namely, Fab 35PA<sub>83</sub>, which neutralizes anthrax toxin. Moreover, a study by Wolf Pérez et al. (76) strongly campaigns for the acceptability of *in silico*-based design and manipulation of therapeutic human mAbs. In fact, by using an *in silico* solubility predictor tool, CamSol, the authors designed 17 variants of a humanized mAb (IgG4) and found a robust correlation between the values predicted *in silico* and obtained by experiments (76). To date, a number of *in silico* studies have been conducted to understand the basic biology of SARS-CoV-2 as well as to propose new intervention strategies against COVID-19. Interestingly, many of them have been validated successfully, which prompted us to imply a similar strategy to screen for the efficacy of various anti-S human mAbs towards SARS-CoV-2 variants and to design a chimeric antibody. Our *in silico* theoretical findings on chimeric mAb has revealed a high degree of efficacy against the newly emerged SARS-CoV-2 variants, and we expect that this chimeric antibody might exert similar functions *in vitro* and *in vivo*.

## CONCLUSION

Both monoclonal and polyclonal antibodies directed against SARS-CoV-2 structural proteins or inflammatory mediators have been employed for treating COVID-19 patients (77). The present study adds a new dimension to the existing knowledge on the efficacy of anti-S protein human mAbs against COVID-19 based on the hypothesis that mAbs could directly bind to the mutant spike proteins of the Alpha and Delta strains of SARS-CoV-2 to neutralize them. Among the 8 human mAbs so far tested against SARS-CoV-2, our *in silico* evidence suggests that tixagevimab, regdanivimab, and cilgavimab could efficiently neutralize most of the B.1.1.7 strains while bamlanivimab, tixagevimab, and sotrovimab could effectively inhibit the Delta variants. Moreover, the concept of chimeric mAb could also be taken into consideration for the treatment of COVID-19 patients infected with the newly emerged strains. However, the limitation of our study is that our findings are theoretical and have not been tested experimentally. Therefore, we welcome further experimental investigation to validate our conclusions, and this will indeed put forward the promising implication of mAb/chimeric mAb-based immunotherapies to combat newly emerging SARS-CoV-2 variants.

## DATA AVAILABILITY STATEMENT

The original contributions presented in the study are included in the article/**Supplementary Material**. Further inquiries can be directed to the corresponding authors.

## AUTHOR CONTRIBUTIONS

Performed the experiments: ND and PC. Analyzed the data: ND, PC, JB, and SM. Wrote the manuscript: JB and SM. Conceived, designed, and supervised the study: JB and SM. All authors contributed to the article and approved the submitted version.

## ACKNOWLEDGMENTS

PC thanks DST, Govt. of India for the award of DST-INSPIRE fellowship. We acknowledge all the open source and globally available databases that were utilized for data mining. BioRender.com used for drawing the illustration is sincerely acknowledged.

## SUPPLEMENTARY MATERIAL

The Supplementary Material for this article can be found online at: <https://www.frontiersin.org/articles/10.3389/fimmu.2021.782506/full#supplementary-material>

## REFERENCES

- Giuntella O, Hyde K, Saccardo S, Sadoff S. Lifestyle and Mental Health Disruptions During COVID-19. *Proc Natl Acad Sci* (2021) 118:e2016632118. doi: 10.1073/PNAS.2016632118
- WHO Coronavirus (COVID-19) Dashboard. *WHO Coronavirus (COVID-19) Dashboard With Vaccination Data*. Available at: <https://covid19.who.int/> (Accessed November 14, 2021).
- Sun Y, Li Y, Wang Y, Jiang D, Liu X. A Future Forecasting for FMCG Firm Performance in Covid-19: An Investigation of Consumer and Business Survival. *Front Public Health* (2021) 9:723084. doi: 10.3389/fpubh.2021.723084
- Das NC, Labala RK, Patra R, Chattoraj A, Mukherjee S. In Silico Identification of New Anti-SARS-CoV-2 Agents From Bioactive Phytocompounds Targeting the Viral Spike Glycoprotein and Human TLR4. *Lett Drug Des Discov* (2021) 18:1–17. doi: 10.2174/1570180818666210901125519
- Varghese PM, Tsolaki AG, Yasmin H, Shastri A, Ferluga J, Vatish M, et al. Host-Pathogen Interaction in COVID-19: Pathogenesis, Potential Therapeutics and Vaccination Strategies. *Immunobiology* (2020) 225:152008. doi: 10.1016/j.imbio.2020.152008
- Huang Y, Yang C, Xu X, Xu W, Liu S. Structural and Functional Properties of SARS-CoV-2 Spike Protein: Potential Antivirus Drug Development for COVID-19. *Acta Pharmacol Sin* 2020 419 (2020) 41:1141–9. doi: 10.1038/s41401-020-0485-4
- Buratto D, Saxena A, Ji Q, Yang G, Pantano S, Zonta F. Rapid Assessment of Binding Affinity of SARS-COV-2 Spike Protein to the Human Angiotensin-Converting Enzyme 2 Receptor and to Neutralizing Biomolecules Based on Computer Simulations. *Front Immunol* (2021) 12:730099. doi: 10.3389/fimmu.2021.730099
- Patra R, Chandra Das N, Mukherjee S. Targeting Human TLRs to Combat COVID-19: A Solution? *J Med Virol* (2021) 93:615–7. doi: 10.1002/jmv.26387
- Choudhury A, Das NC, Patra R, Mukherjee S. In Silico Analyses on the Comparative Sensing of SARS-CoV-2 mRNA by the Intracellular TLRs of Humans. *J Med Virol* (2021) 93:2476–86. doi: 10.1002/jmv.26776
- Choudhury A, Das NC, Patra R, Bhattacharya M, Ghosh P, Patra BC, et al. Exploring the Binding Efficacy of Ivermectin Against the Key Proteins of SARS-CoV-2 Pathogenesis: An in Silico Approach. *Future Virol* (2021) 16:277–91. doi: 10.2217/FVL-2020-0342
- Saldanha-Araujo F, Melgaço Garcez E, Silva-Carvalho AE, Carvalho JL. Mesenchymal Stem Cells: A New Piece in the Puzzle of COVID-19 Treatment. *Front Immunol* (2020) 11:1563. doi: 10.3389/fimmu.2020.01563
- Tracking SARS-CoV-2 Variants. Available at: <https://www.who.int/en/activities/tracking-SARS-CoV-2-variants/> (Accessed November 14, 2021).
- Callaway E. The Coronavirus is Mutating - Does it Matter? *Nature* (2020) 585:174–7. doi: 10.1038/D41586-020-02544-6
- Tada T, Zhou H, Dcosta BM, Samanovic MI, Mulligan MJ, Landau NR. The Spike Proteins of SARS-CoV-2 B.1.617 and B.1.618 Variants Identified in India Provide Partial Resistance to Vaccine-Elicited and Therapeutic Monoclonal Antibodies. *bioRxiv* (2021) 444076. doi: 10.1101/2021.05.14.444076
- Harvey WT, Carabelli AM, Jackson B, Gupta RK, Thomson EC, Harrison EM, et al. SARS-CoV-2 Variants, Spike Mutations and Immune Escape. *Nat Rev Microbiol* 2021 197 (2021) 19:409–24. doi: 10.1038/s41579-021-00573-0
- Hoffmann M, Hofmann-Winkler H, Krüger N, Kempf A, Nehlmeier I, Graichen L, et al. SARS-CoV-2 Variant B.1.617 Is Resistant to Bamlanivimab and Evades 1 Antibodies Induced by Infection and Vaccination. *bioRxiv* (2021) 442663. doi: 10.1101/2021.05.04.442663
- COVID-19 Weekly Epidemiological Update. Available at: [https://www.who.int/docs/default-source/coronaviruse/situation-reports/20210511\\_weekly\\_epi\\_update\\_39.pdf](https://www.who.int/docs/default-source/coronaviruse/situation-reports/20210511_weekly_epi_update_39.pdf) (Accessed July 20, 2021).
- Dhar MS, Marwal R, Radhakrishnan VS, Ponnusamy K, Jolly B, Bhojar RC, et al. Genomic Characterization and Epidemiology of an Emerging SARS-CoV-2 Variant in Delhi, India. *medRxiv* (2021) 21258076. doi: 10.1101/2021.06.02.21258076
- Planas D, Veyer D, Baidaliuk A, Staropoli I, Guivel-Benhassine F, Rajah MM, et al. Reduced Sensitivity of Infectious SARS-CoV-2 Variant B.1.617.2 to Monoclonal Antibodies and Sera From Convalescent and Vaccinated Individuals. *bioRxiv* (2021) 445838. doi: 10.1101/2021.05.26.445838
- Dube T, Ghosh A, Mishra J, Kompella UB, Panda JJ. Repurposed Drugs, Molecular Vaccines, Immune-Modulators, and Nanotherapeutics to Treat and Prevent COVID-19 Associated With SARS-CoV-2, a Deadly Nanovector. *Adv Ther* (2020) 4:2000172. doi: 10.1002/adtp.202000172
- Taylor PC, Adams AC, Hufford MM, de la Torre I, Winthrop K, Gottlieb RL. Neutralizing Monoclonal Antibodies for Treatment of COVID-19. *Nat Rev Immunol* (2021) 21:382–93. doi: 10.1038/s41577-021-00542-x
- Vojdani A, Vojdani E, Kharrazian D. Reaction of Human Monoclonal Antibodies to SARS-CoV-2 Proteins With Tissue Antigens: Implications for Autoimmune Diseases. *Front Immunol* (2021) 11:617089. doi: 10.3389/fimmu.2020.617089
- Fagre AC, Manhard J, Adams R, Eckley M, Zhan S, Lewis J, et al. A Potent SARS-CoV-2 Neutralizing Human Monoclonal Antibody That Reduces Viral Burden and Disease Severity in Syrian Hamsters. *Front Immunol* (2020) 11:614256. doi: 10.3389/fimmu.2020.614256
- Gupta A, Gonzalez-Rojas Y, Juarez E, Casal MC, Moya J, Falci DR, et al. Early Covid-19 Treatment With SARS-CoV-2 Neutralizing Antibody Sotrovimab. *medRxiv* (2021) 21257096. doi: 10.1101/2021.05.27.21257096
- Drugs.com. Update on AZD7442 STORM CHASER Trial in Post-Exposure Prevention of Symptomatic COVID-19 (2021). Available at: [https://www.drugs.com/clinical\\_trials/update-azd7442-storm-chaser-trial-post-exposure-prevention-symptomatic-covid-19-19437.html](https://www.drugs.com/clinical_trials/update-azd7442-storm-chaser-trial-post-exposure-prevention-symptomatic-covid-19-19437.html) (Accessed August 15, 2021).
- Chen J, Gao K, Wang R, Wei G-W. Revealing the Threat of Emerging SARS-CoV-2 Mutations to Antibody Therapies. *bioRxiv* (2021) 439473. doi: 10.1101/2021.04.12.439473
- Raybould MIJ, Kovaltsuk A, Marks C, Deane CM. CoV-AbDab: The Coronavirus Antibody Database. *Bioinformatics* (2021) 37:734–5. doi: 10.1093/bioinformatics/btaa739
- Waterhouse A, Bertoni M, Bienert S, Studer G, Tauriello G, Gumienny R, et al. SWISS-MODEL: Homology Modelling of Protein Structures and Complexes. *Nucleic Acids Res* (2018) 46:W296–303. doi: 10.1093/NAR/GKY427
- Dunbar J, Krawczyk K, Leem J, Marks C, Nowak J, Regep C, et al. SABPred: A Structure-Based Antibody Prediction Server. *Nucleic Acids Res* (2016) 44:W474–8. doi: 10.1093/nar/gkw361
- Leem J, Dunbar J, Georges G, Shi J, Deane CM. ABodyBuilder: Automated Antibody Structure Prediction With Data-Driven Accuracy Estimation. *MAbs* (2016) 8:1259–68. doi: 10.1080/19420862.2016.1205773
- Krawczyk K, Baker T, Shi J, Deane CM. Antibody I-Patch Prediction of the Antibody Binding Site Improves Rigid Local Antibody-Antigen Docking. *Protein Eng Des Sel* (2013) 26:621–9. doi: 10.1093/protein/gzt043
- Norman RA, Ambrosetti F, Bonvin AMJJ, Colwell LJ, Kelm S, Kumar S, et al. Computational Approaches to Therapeutic Antibody Design: Established Methods and Emerging Trends. *Brief Bioinform* (2020) 21:1549–67. doi: 10.1093/bib/bbz095
- Krawczyk K, Liu X, Baker T, Shi J, Deane CM. Improving B-Cell Epitope Prediction and its Application to Global Antibody-Antigen Docking. *Bioinformatics* (2014) 30:2288–94. doi: 10.1093/bioinformatics/btu190
- Lüthy R, Bowie JU, Eisenberg D. Assessment of Protein Models With Three-Dimensional Profiles. *Nature* (1992) 356:83–5. doi: 10.1038/356083a0
- Bowie JU, Lüthy R, Eisenberg D. A Method to Identify Protein Sequences That Fold Into a Known Three-Dimensional Structure. *Science* (80-) (1991) 253:164–70. doi: 10.1126/science.1853201
- Van Zundert GCP, Rodrigues JPGLM, Trellet M, Schmitz C, Kastrius PL, Karaca E, et al. The HADDOCK2.2 Web Server: User-Friendly Integrative Modeling of Biomolecular Complexes. *J Mol Biol* (2016) 428:720–5. doi: 10.1016/j.jmb.2015.09.014
- Das NC, Patra R, Gupta PSS, Ghosh P, Bhattacharya M, Rana MK, et al. Designing of a Novel Multi-Epitope Peptide Based Vaccine Against Brugia Malayi: An in Silico Approach. *Infect Genet Evol* (2021) 87:104633. doi: 10.1016/j.meegid.2020.104633
- López-Blanco JR, Aliaga JI, Quintana-Ortí ES, Chacón P. iMODS: Internal Coordinates Normal Mode Analysis Server. *Nucleic Acids Res* (2014) 42:W271–6. doi: 10.1093/nar/gku339
- Das NC, Sen Gupta PS, Biswal S, Patra R, Rana MK, Mukherjee S. In-Silico Evidence of Filarial Cystatin as a Putative Ligand of Human TLR4. *J Biomol Struct Dyn* (2021) 39:1–17. doi: 10.1080/07391102.2021.1918252
- Xue LC, Rodrigues JP, Kastrius PL, Bonvin AM, Vangone A. PRODIGY: A Web Server for Predicting the Binding Affinity of Protein-Protein Complexes. *Bioinformatics* (2016) 32:3676–8. doi: 10.1093/BIOINFORMATICS/BTW514
- Raybould MIJ, Marks C, Krawczyk K, Taddese B, Nowak J, Lewis AP, et al. Five Computational Developability Guidelines for Therapeutic Antibody Profiling. *Proc Natl Acad Sci* (2019) 116:4025–30. doi: 10.1073/pnas.1810576116

42. Zhao J, Nussinov R, Wu W-J, Ma B. In Silico Methods in Antibody Design. *Antibodies* (2018) 7:22. doi: 10.3390/antib7030022
43. Ambrosetti F, Jandova Z, Bonvin AMJJ. *A Protocol for Information-Driven Antibody-Antigen Modelling With the HADDOCK2.4 Webserver* (2020). Available at: <https://arxiv.org/abs/2005.03283v1> (Accessed July 20, 2021).
44. Choudhury A, Mukherjee S. In Silico Studies on the Comparative Characterization of the Interactions of SARS-CoV-2 Spike Glycoprotein With ACE-2 Receptor Homologs and Human TLRs. *J Med Virol* (2020) 92:2105–13. doi: 10.1002/jmv.25987
45. Wang P, Nair MS, Liu L, Iketani S, Luo Y, Guo Y, et al. Antibody Resistance of SARS-CoV-2 Variants B.1.351 and B.1.1.7. *Nature* (2021) 593:130–5. doi: 10.1038/s41586-021-03398-2
46. Singh J, Rahman SA, Ehtesham NZ, Hira S, Hasnain SE. SARS-CoV-2 Variants of Concern are Emerging in India. *Nat Med* (2021) 27:1131–3. doi: 10.1038/s41591-021-01397-4
47. Anka AU, Tahir MI, Abubakar SD, Alsabbagh M, Zian Z, Hamedifar H, et al. Coronavirus Disease 2019 (COVID-19): An Overview of the Immunopathology, Serological Diagnosis and Management. *Scand J Immunol* (2021) 93:e12998. doi: 10.1111/SJL.12998
48. Chen P, Nirula A, Heller B, Gottlieb RL, Boscia J, Morris J, et al. SARS-CoV-2 Neutralizing Antibody LY-CoV555 in Outpatients With Covid-19. *N Engl J Med* (2020) 384:229–37. doi: 10.1056/NEJMoa2029849
49. Weinreich DM, Sivapalasingam S, Norton T, Ali S, Gao H, Bhoire R, et al. REGN-COV2, a Neutralizing Antibody Cocktail, in Outpatients With Covid-19. *N Engl J Med* (2021) 384:238–51. doi: 10.1056/NEJMoa2035002
50. Gottlieb RL, Nirula A, Chen P, Boscia J, Heller B, Morris J, et al. Effect of Bamlanivimab as Monotherapy or in Combination With Etesevimab on Viral Load in Patients With Mild to Moderate COVID-19: A Randomized Clinical Trial. *JAMA* (2021) 325:632–44. doi: 10.1001/jama.2021.0202
51. *Coronavirus (COVID-19) Update: FDA Revokes Emergency Use Authorization for Monoclonal Antibody Bamlanivimab*. FDA. Available at: <https://www.fda.gov/news-events/press-announcements/coronavirus-covid-19-update-fda-revokes-emergency-use-authorization-monoclonal-antibody-bamlanivimab> (Accessed August 1, 2021).
52. *Coronavirus (COVID-19) Update: FDA Authorizes Additional Monoclonal Antibody for Treatment of COVID-19*. FDA. Available at: <https://www.fda.gov/news-events/press-announcements/coronavirus-covid-19-update-fda-authorizes-additional-monoclonal-antibody-treatment-covid-19> (Accessed August 1, 2021).
53. Ryu D-K, Woo H-M, Kang B, Noh H, Kim J-I, Seo J-M, et al. The *In Vitro* and *In Vivo* Potency of CT-P59 Against Delta and its Associated Variants of SARS-CoV-2. *bioRxiv* (2021) 453472. doi: 10.1101/2021.07.23.453472
54. Ryu DK, Song R, Kim M, Kim Y, Kim C, Kim JI, et al. Therapeutic Effect of CT-P59 Against SARS-CoV-2 South African Variant. *Biochem Biophys Res Commun* (2021) 566:135–40. doi: 10.1016/j.bbrc.2021.06.016
55. Kim C, Ryu D-K, Lee J, Kim Y-I, Seo J-M, Kim Y-G, et al. A Therapeutic Neutralizing Antibody Targeting Receptor Binding Domain of SARS-CoV-2 Spike Protein. *Nat Commun* (2021) 12:288. doi: 10.1038/s41467-020-20602-5
56. Qaraghuli MM Al, Kubiak-Ossowska K, Ferro VA, Mulheran PA. Antibody-Protein Binding and Conformational Changes: Identifying Allosteric Signalling Pathways to Engineer a Better Effector Response. *Sci Rep* 2020 101 (2020) 10:1–10. doi: 10.1038/s41598-020-70680-0
57. Martín-Galiano AJ, McConnell MJ. Using Omics Technologies and Systems Biology to Identify Epitope Targets for the Development of Monoclonal Antibodies Against Antibiotic-Resistant Bacteria. *Front Immunol* (2019) 10:2841. doi: 10.3389/fimmu.2019.02841
58. Kumar S, Chandele A, Sharma A. Current Status of Therapeutic Monoclonal Antibodies Against SARS-CoV-2. *PLoS Pathog* (2021) 17:e1009885. doi: 10.1371/journal.ppat.1009885
59. Lei C, Qian K, Li T, Zhang S, Fu W, Ding M, et al. Neutralization of SARS-CoV-2 Spike Pseudotyped Virus by Recombinant ACE2-Ig. *Nat Commun* (2020) 11:2070. doi: 10.1038/s41467-020-16048-4
60. Hsueh C, Plotkin SS. Rationally Designed Chimeric Antibodies for COVID-19 and Future Coronavirus Variants. *Biophys J* (2021) 120:21a–a. doi: 10.1016/j.bpj.2020.11.390
61. Do P-C, Nguyen TH, Vo UHM, Le L. iBRAB: In Silico Based-Designed Broad-Spectrum Fab Against H1N1 Influenza A Virus. *PLoS One* (2021) 15:e0239112. doi: 10.1371/journal.pone.0239112
62. Shey RA, Ghogomu SM, Esoh KK, Nebangwa ND, Shintouo CM, Nongley NF, et al. In-Silico Design of a Multi-Epitope Vaccine Candidate Against Onchocerciasis and Related Filarial Diseases. *Sci Rep* (2019) 9:4409. doi: 10.1038/s41598-019-40833-x
63. Bhatia V, Sinha M, Luxon B, Garg N. Utility of the Trypanosoma Cruzi Sequence Database for Identification of Potential Vaccine Candidates by in Silico and *In Vitro* Screening. *Infect Immun* (2004) 72:6245–54. doi: 10.1128/IAI.72.11.6245-6254.2004
64. Duarte A, Queiroz ATL, Tosta R, Carvalho AM, Barbosa CH, Bellio M, et al. Prediction of CD8+ Epitopes in Leishmania Braziliensis Proteins Using EPIBOT: In Silico Search and *In Vivo* Validation. *PLoS One* (2015) 10:e0124786. doi: 10.1371/journal.pone.0124786
65. Hasanazadeh S, Habibi M, Shokrgozar MA, Ahangari Cohan R, Ahmadi K, Asadi Karam MR, et al. In Silico Analysis and *In Vivo* Assessment of a Novel Epitope-Based Vaccine Candidate Against Uropathogenic Escherichia Coli. *Sci Rep* (2020) 10:16258. doi: 10.1038/s41598-020-73179-w
66. Hegde NR, Gauthami S, Sampath Kumar HM, Bayry J. The Use of Databases, Data Mining and Immunoinformatics in Vaccinology: Where are We? *Expert Opin Drug Discov* (2018) 13:117–30. doi: 10.1080/17460441.2018.1413088
67. Kalita P, Padhi A, Zhang KYJ, Tripathi T. Design of a Peptide-Based Subunit Vaccine Against Novel Coronavirus SARS-CoV-2. *Microb Pathog* (2020) 145:104236. doi: 10.1016/j.micpath.2020.104236
68. Narula A, Pandey RK, Khatoun N, Mishra A, Prajapati VK. Excavating Chikungunya Genome to Design B and T Cell Multi-Epitope Subunit Vaccine Using Comprehensive Immunoinformatics Approach to Control Chikungunya Infection. *Infect Genet Evol* (2018) 61:4–15. doi: 10.1016/j.meegid.2018.03.007
69. Panda PK, Arul MN, Patel P, Verma SK, Luo W, Rubahn H-G, et al. Structure-Based Drug Designing and Immunoinformatics Approach for SARS-CoV-2. *Sci Adv* (2020) 6:eabb8097. doi: 10.1126/sciadv.abb8097
70. Arega AM, Pattanaik KP, Nayak S, Mahapatra RK. Computational Discovery and *Ex-Vivo* Validation Study of Novel Antigenic Vaccine Candidates Against Tuberculosis. *Acta Trop* (2021) 217:105870. doi: 10.1016/j.actatropica.2021.105870
71. Das NC, Ray AS, Bayry J, Mukherjee S. Therapeutic Efficacy of Anti-Bestrophin Antibodies Against Experimental Filariasis: Immunological, Immune-Informatics and Immune Simulation Investigations. *Antibodies* (2021) 10:14. doi: 10.3390/antib10020014
72. Yuan S, Chan JF-W, den-Haan H, Chik KK-H, Zhang AJ, Chan CC-S, et al. Structure-Based Discovery of Clinically Approved Drugs as Zika Virus NS2B-NS3 Protease Inhibitors That Potently Inhibit Zika Virus Infection *In Vitro* and *In Vivo*. *Antiviral Res* (2017) 145:33–43. doi: 10.1016/j.antiviral.2017.07.007
73. Nyárady Z, Czömpöly T, Bösze S, Nagy G, Petrohai Á, Pál J, et al. Validation of in Silico Prediction by *In Vitro* Immunoserological Results of Fine Epitope Mapping on Citrate Synthase Specific Autoantibodies. *Mol Immunol* (2006) 43:830–8. doi: 10.1016/j.molimm.2005.06.044
74. Memarnejadian A, Roohvand F, Arashkia A, Rafati S, Shokrgozar MA. Polytope DNA Vaccine Development Against Hepatitis C Virus: A Streamlined Approach from in Silico Design to *In Vitro* and Primary *In Vivo* Analyses in BALB/c Mice. *Protein Pept Lett* (2009) 16:842–50. doi: 10.2174/092986609788681788
75. Pelat T, Bedouelle H, Rees AR, Crennell SJ, Lefranc M-P, Thullier P. Germline Humanization of a Non-Human Primate Antibody That Neutralizes the Anthrax Toxin, by *In Vitro* and *In Silico* Engineering. *J Mol Biol* (2008) 384:1400–7. doi: 10.1016/j.jmb.2008.10.033
76. Wolf Pérez A-M, Sormanni P, Andersen JS, Sakhnini LI, Rodriguez-Leon I, Bjelke JR, et al. *In Vitro* and *In Silico* Assessment of the Developability of a Designed Monoclonal Antibody Library. *MAbs* (2019) 11:388–400. doi: 10.1080/19420862.2018.1556082
77. Bonam SR, Kaveri SV, Sakuntabhai A, Gilardin L, Bayry J. Adjunct Immunotherapies for the Management of Severely Ill COVID-19 Patients. *Cell Rep Med* (2020) 1:100016. doi: 10.1016/j.xcrm.2020.100016

**Conflict of Interest:** The authors declare that the research was conducted in the absence of any commercial or financial relationships that could be construed as a potential conflict of interest.

**Publisher's Note:** All claims expressed in this article are solely those of the authors and do not necessarily represent those of their affiliated organizations, or those of the publisher, the editors and the reviewers. Any product that may be evaluated in

this article, or claim that may be made by its manufacturer, is not guaranteed or endorsed by the publisher.

Copyright © 2022 Das, Chakraborty, Bayry and Mukherjee. This is an open-access article distributed under the terms of the Creative Commons Attribution License

(CC BY). The use, distribution or reproduction in other forums is permitted, provided the original author(s) and the copyright owner(s) are credited and that the original publication in this journal is cited, in accordance with accepted academic practice. No use, distribution or reproduction is permitted which does not comply with these terms.